FISEVIER

Contents lists available at ScienceDirect

# International Journal of Biological Macromolecules

journal homepage: www.elsevier.com/locate/ijbiomac





# Antler thymosin $\beta10$ reduces liver fibrosis via inhibiting TGF- $\beta1/$ SMAD pathway

Guokun Zhang  $^{a,1}$ , Liyan Shi  $^{b,1}$ , Jiping Li  $^{a,1}$ , Jing Ren  $^{a,c}$ , Dongxu Wang  $^{a}$ , Xin Guo  $^{a}$ , Qianqian Guo  $^{a,*}$ , Chunyi Li  $^{a,c,**}$ 

- <sup>a</sup> Institute of Antler Science and Product Technology, Changchun Sci-Tech University; 130600 Changchun, China
- <sup>b</sup> The Third Hospital of Jilin University, 130033 Changchun, China
- <sup>c</sup> College of Chinese Medicinal Materials, Jilin Agricultural University, 130118 Changchun, China

### ARTICLE INFO

### Keywords: Thymosin β10 Liver fibrosis HSC activation

### ABSTRACT

Hepatic stellate cell (HSC) activation is a crucial step in the development of liver fibrosis. Previous studies have shown that antler stem cells (AnSCs) inhibited HSC activation, suggesting that this may be achieved through secreting or releasing peptides. This study aimed to investigate whether AnSC-derived peptides (AnSC-P) could reduce liver fibrosis. The results showed that AnSC-P effectively reduced liver fibrosis in rats. Furthermore, we found that thymosin  $\beta$ 10 (T $\beta$ -10) was rich in AnSC-P, which may be the main component of AnSC-P contributing to the reduction in liver fibrosis. A further study showed that T $\beta$ -10 reduced liver fibrosis in rats, with a reduction in HYP and MDA levels in the liver tissues, a decrease in the serum levels of ALP, ALT, AST, and TBIL and an increase in TP and ALB. Moreover, T $\beta$ -10 decreased the expression levels of the genes related to the TGF- $\beta$ /SMAD signaling pathway in vivo. In addition, T $\beta$ -10 also inhibited TGF- $\beta$ 1-induced HSC activation and decreased the expression levels of the TGF- $\beta$ /SMAD signaling pathway-related genes in HSCs in vitro. In conclusion, antler T $\beta$ -10 is a potential drug candidate for the treatment of liver fibrosis, the effect of which may be achieved via inhibition of the TGF $\beta$ /SMAD signaling pathway.

# 1. Introduction

Liver fibrosis is a common scarring response to chronic liver diseases, including viral and autoimmune hepatitis, alcohol and nonalcoholic fatty liver syndromes, and biliary obstruction disease [1,2]. The essential feature of liver fibrosis is the excessive accumulation of extracellular matrix (ECM) mainly produced by hepatic stellate cells (HSCs) [1,2]. HSCs remain quiescent in healthy livers [3], but are activated to transdifferentiate into myofibroblasts via repeated injuries to the liver which results in the expression of gene pathways for the synthesis of  $\alpha$  smooth muscle actin ( $\alpha$ -SMA) and collagen I [4,5]. Excessive levels of transforming growth factor- $\beta$ 1 (TGF- $\beta$ 1) activity in the liver have been associated with HSC activation and proliferation [6]. In this respect, SMAD2/3, after being stimulated by TGF- $\beta$ 1, become phosphorylated and oligomerized with SMAD4, and was then translocated to the nucleus to regulate expression of the TGF- $\beta$ 1 targeted genes in the activated HSCs [7,8]. Therefore, inhibition of TGF- $\beta$ 1/SMAD pathway could

suppress HSC activation, which may represent an effective target therapy for liver fibrosis.

Recently, mesenchymal stem cell (MSC) transplantation has been proven to be an effective way to stimulate tissue and organ regeneration, both clinically and in animal experiments, through secretion of or release of components after homing to the site of tissue damage [9,10]. Deer antler stem cells (AnSCs) are a novel type of adult MSCs with the partial properties of embryonic stem cells, which support the annual full regeneration of deer antlers from the pedicle [11,12]. The first step in antler regeneration is the scarless (nonfibrotic) wound healing over the pedicle (permanent bony protuberance) stump following the casting of the previous hard antler [12,13]. This process depends on the AnSCs in the adjacent antler blastema [13]. This ability of AnSCs to promote scarless wound healing can also be realized in other species if xenogeneically transplanted, such as rats [14–17]. Such therapeutic effects of AnSCs are due to their potent anti-fibrotic activities. Therefore, we considered the possibility that AnSCs might have therapeutic potential

<sup>\*</sup> Corresponding author.

<sup>\*\*</sup> Correspondence to: C. Li, Institute of Antler Science and Product Technology, Changchun Sci-Tech University, 1345 Pudong Rd., 130600 Changchun, China. E-mail addresses: gqqice@163.com (Q. Guo), lichunyi1959@163.com (C. Li).

 $<sup>^{\</sup>rm 1}$  These authors contributed equally: Guokun Zhang, Liyan Shi, and Jiping Li.

in treating internal organ fibrosis, and our recent study has confirmed our hypothesis, with the successful use of the AnSC treatment in reducing both pulmonary fibrosis [18] and liver fibrosis [19]. However, considering the potential risks of direct transplantation of xenogeneic animal stem cells to human body, it is necessary to identify the specific components of AnSCs that are anti-fibrotic.

In the present study, we investigated the effects of AnSC-derived peptides (AnSC-P) and their main component, thymosin  $\beta10$  (T $\beta$ -10), on liver fibrosis using CCl<sub>4</sub>-induced rats and TGF- $\beta$ 1-induced HSC activation. We found that AnSC-P effectively reduced liver fibrosis, which may be achieved mainly through T $\beta$ -10, one of the main components of AnSC-P. Further study found that T $\beta$ -10 inhibited the TGF- $\beta$ 1/SMAD signaling pathway in vivo and in vitro. Therefore, our results strongly suggest that T $\beta$ -10 is an essential component of AnSC-P for reducing liver fibrosis, which may be achieved via inhibiting the TGF- $\beta$ 1/SMAD signaling pathway using AnSC-derived peptides.

#### 2. Materials and methods

# 2.1. Preparation of AnSC-P and $T\beta$ -10

AnSCs were cultured in a DMEM medium containing 10 % FBS, and when density reached 80 %, the medium was replaced with Ultra-CULTURE serum-free medium (Lonza, USA) for 48 h. The cells and conditioned medium were collected for AnSC-P preparation. Specifically, the sample was dissociated ultrasonically in the ice box for 2 s/time, with intervals of 3 s, and a duration of 10 min. The samples were filtered through a 0.22  $\mu m$  pore-size membrane and then freeze-dried in a vacuum freeze-dryer. The freeze-dried powder (AnSC-P) was stored at  $-20~^{\circ} C$ . Rat bone marrow mesenchymal stem cell-derived peptides (BMSC-P) were prepared using the same procedure as the AnSC-P. Briefly, BMSCs were cultured in a DMEM medium and then replaced with a serum-free medium for 48 h. Further, BMSCs and conditioned medium were collected for BMSC-P preparation.

Antler  $T\beta$ -10 was synthesized via solid-phase peptide synthesis and obtained the following amino acid sequence "MADKPDMGEINSFD-KAKLKKTETQEKNTLPTKETIEQEKQAK", which is identical to the previously reported one [20]. The proteins were purified through high-performance liquid chromatography (Purity >98.00 %).

# 2.2. Animal model and treatment

Eight-week-old female SD rats were purchased from Liaoning Changsheng Biotechnology Co., Ltd. (Benxi, China). All manipulations on experimental rats were performed under the guidelines and study protocols of the Animal Ethics Committee of Changchun Sci-Tech University (Ethics number: CKARI202006).

In total, 56 rats (7 rats by 8 groups) were injected with  $CCl_4$  (diluted 1:1 in olive oil; 0.5 ml of  $CCl_4$ /kg body weight) intraperitoneally twice a week for 8 weeks [21,22]. Control rats (14 with 7 rats by 2 groups) were treated in the same way but using olive oil only.

1) AnSC-P:  $CCl_4$ -treated rats were injected intravenously at 1.0 mg/kg AnSC-P (twice a week) for 4 weeks, with BMSC-P and PBS as the positive and negative controls, respectively.

Our previous study showed that  $1\times 10^6$  AnSCs/rat treatment (intravenous, once/week) significantly reduced liver fibrosis in CCl<sub>4</sub>-induced rats [19]. Therefore, in vivo experiments, we cultured this amount of AnSCs (4th passage) in serum-free DMEM medium for 48 h, freeze-dried the cells and medium, and then weighed the left-over dry material (0.5 mg). Overall, the dose of AnSC-P treatment was equivalent to approximately 1 mg/kg ( $\approx 0.25$  mg/rat  $\times$  twice/week).

2) T $\beta$ -10: CCl<sub>4</sub>-treated rats were injected intravenously at 0.5 and 1.0 mg/kg T $\beta$ -10 (twice a week) for 4 weeks, respectively. PBS was used as the negative control.

Rat blood samples from each animal were taken from the heart by using a syringe needle directly penetrating the chest into heart chambers

under general anesthesia, and the serum was stored at  $-70~^\circ\text{C}$  for subsequent liver function assay. The collected livers were divided into three parts as below:

- 1) preserved in 4 % paraformaldehyde for histological examination;
- immediately used for assays of hydroxyproline (HYP) and malonaldehyde (MDA);
- 3) frozen at -70 °C for protein and RNA extraction.

# 2.3. Histological examination

Liver tissue imbedded in paraffin wax was cut at  $4.0~\mu m$  and stained with hematoxylin-eosin, Sirius Red and Masson's trichrome, were used for examination of the general structure and the collagen distribution, respectively.

Immunohistochemical (IHC) localizations for different factors were performed according to the manufacturer's instructions (MXB, Fuzhou, China). Briefly, paraffin sections of liver tissue samples were rehydrated and subjected to antigen retrieval in 10 mM sodium citrate buffer (pH 6.0), incubated in 10 % goat serum for 0.5 h and followed by avidinbiotin block; subsequently incubated with anti-PCNA (ProteinTech, 60097-1-Ig, Wuhan, China, 1: 500 dilution), anti-TGF- $\beta$ 1 (Bioss, bsm-33345M, Beijing, China 1: 500 dilution), anti- $\alpha$ -SMA (ProteinTech, 14395-1-AP, Wuhan, China, 1: 500 dilution), respectively, at 4 °C overnight. On the next day, the sections were incubated with the sections were examined and photographed under a microscope, and the proportion of positively (+) stained cells to total number of cells was calculated.

#### 2.4. Assays of liver function parameters

Liver function parameters were analyzed using serum samples via Beckman Coulter AU480 Biochemical Analysis System; these included total protein (TP), albumin (ALB), alkaline phosphatase (ALP), alanine aminotransferase (ALT), aspartate aminotransferase (AST) and total bilirubin (TBIL). The kits for these analyses were purchased from Biosino Bio-Technology and Science Inc. (Beijing, China).

# 2.5. HYP and MDA assay

Concentrations of HYP and MDA in liver tissue were measured using the spectrophotometric method with assay kits according to the manufacturer's instructions (Nanjing Jiancheng Biological Engineering Institute Co., Ltd., Nanjing, China).

# 2.6. Cell culture and treatment

The rat hepatic stellate cell (HSC) line was purchased from Beijing Ding Guo Biotechnology Co., Ltd. (Beijing, China). HSCs were cultured in the culture medium: Dulbecco's Modified Eagle Medium (Gibco, NY, USA) supplemented with 100 U/ml penicillin, 100  $\mu g/ml$  streptomycin and 10 % fetal bovine serum (HyClone, Beijing, China), in a humidified incubator with 5 % (v/v) CO $_2$  atmosphere at 37 °C. HSCs were cultured for 48 h with TGF- $\beta 1$  (5 ng/ml) to induce activation; some of the cells were also treated with T $\beta$ -10 (100 ng/ml, the screening of the optimal concentration is shown in Fig. S1) as indicated; then the expression of  $\alpha$ -SMA was measured using immunofluorescence staining, and the expression levels of TGF- $\beta 1/S$ MAD signaling pathway-related genes were detected using qRT-PCR and western blot assay.

# 2.7. Immunofluorescence staining

HSCs were cultured in a 24-well-plate (50,000 Cells/well) till 80 % confluence, and then fixed in 4 % paraformaldehyde for 30 min, treated with 0.2 % Triton X-100 for 10 min. Expression levels of  $\alpha$ -SMA in the

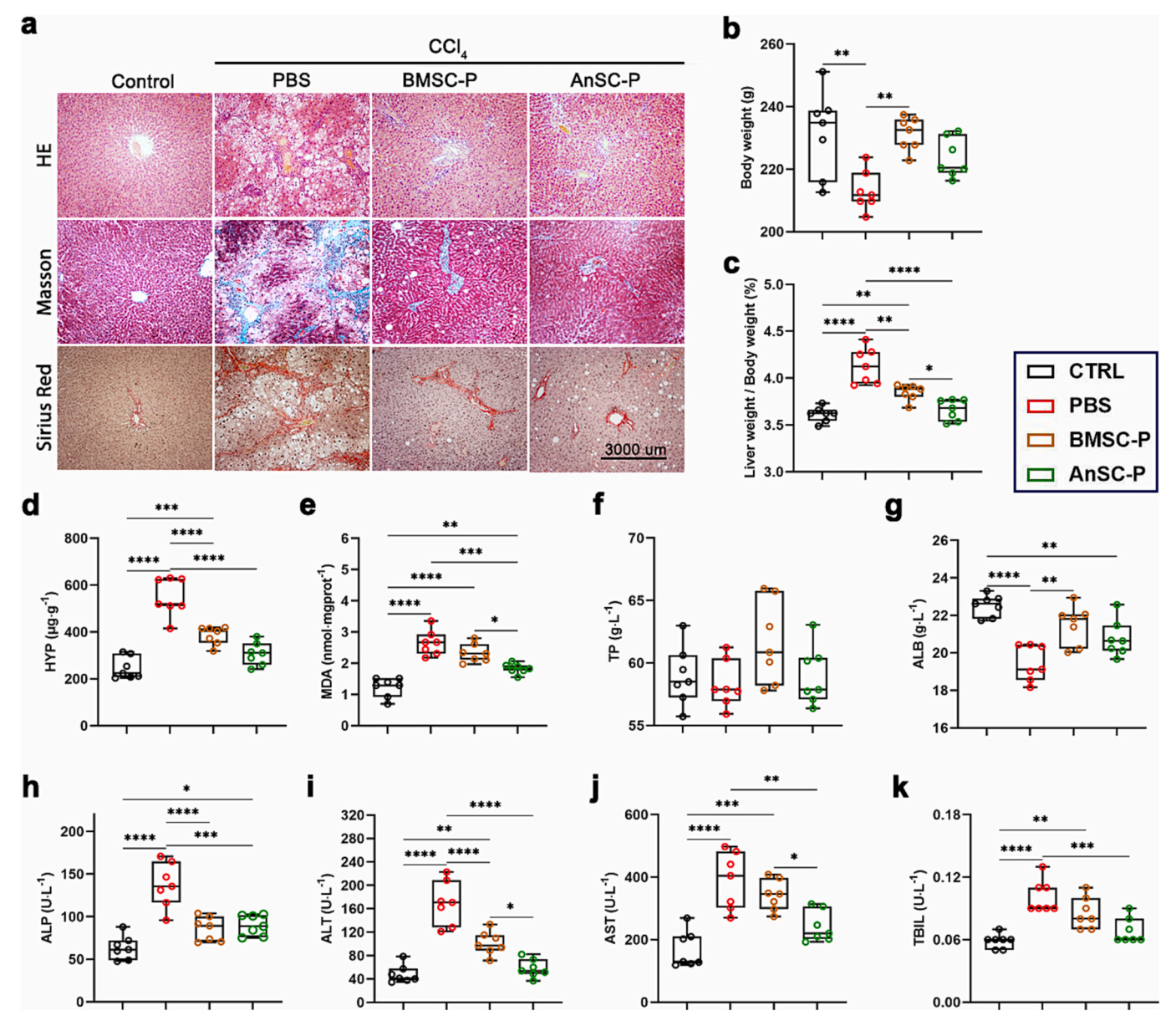


**Fig. 1.** Effects of AnSC-P on rat liver fibrosis induced by CCl<sub>4</sub>. CCl<sub>4</sub> was given via intraperitoneal injection twice/week for eight weeks. AnSC-P was treated via intravenous injection once/week after CCl<sub>4</sub> treatment for four weeks. Rats were randomly allocated into 4 groups (7 rats/group): Control, PBS, BMSC-P, AnSC-P. (a) Photomicrographs of liver sections with staining of HE, Masson or Sirius Red; scale bar = 3000  $\mu$ m. (b) Bodyweight. (c) Liver weight/bodyweight. (d,e) Concentration of liver HYP and MDA. (f-k) Serum biochemical parameters (TP, ALB, ALP, ALT, AST, and TBIL) related to liver function. Note that AnSC-P treatment significantly suppressed liver fibrosis and improved liver function compared with the PBS group, and there was a strong trend for AnSC that had a better effect on suppressing liver fibrosis than BMSC-P. Value: mean  $\pm$  s.e.m.; \*p < 0.05, \*p < 0.01, and \*p < 0.001 by one-way ANOVA. Abbreviation: BMSC-P, bone mesenchymal stem cell-derived peptides; AnSC-P, antler stem cell-derived peptides; HYP, hydroxyproline; MDA, malondialdehyde; TP, Total protein; ALB, Albumin; ALP, Alkaline phosphatase; ALT, Alanine aminotransferase; AST, Aspartate aminotransferase; and TBIL, Total bilirubin. (For interpretation of the references to color in this figure legend, the reader is referred to the web version of this article.)

HSCs were measured using a kit (ProteinTech, 14395-1-AP, Wuhan, China, 1: 500 dilution).

AnSCs were cultured in a 24-well plate (50,000 Cells/well) till 80 % confluence, and then fixed in 4 % paraformaldehyde for 30 min, treated with 0.2 % Triton X-100 for 10 min. Expression levels of T $\beta$ -10 in the HSCs were measured using a kit (Abcom, ab14338, USA, 1: 1000 dilution). The concentration of T $\beta$ -10 in the medium was measured via ELISA assay.

# 2.8. RNA extraction and qRT-PCR analysis

Total RNA was extracted from the liver tissues or HSCs using TRIzol

reagent (Roche Diagnostics, Indianapolis, IN) as described by the manufacturer. Single-stranded cDNA was synthesized using 0.5  $\mu g$  of oligo (dT) primer and 2  $\mu g$  of total RNA via reverse transcription. PCR was performed at 94  $^{\circ}$ C for 30 s, 58  $^{\circ}$ C for 1 min and 72  $^{\circ}$ C for 1 min. The primers used for quantitative PCR are listed in Table 1.

# 2.9. Western blot analysis

Proteins were extracted from the liver tissues or HSCs using RAPI buffer. The extracted proteins were separated using polyacrylamide SDS gel and electrophoretically transferred onto polyvinylidene fluoride membranes (Millipore, MA). The membranes were probed with the

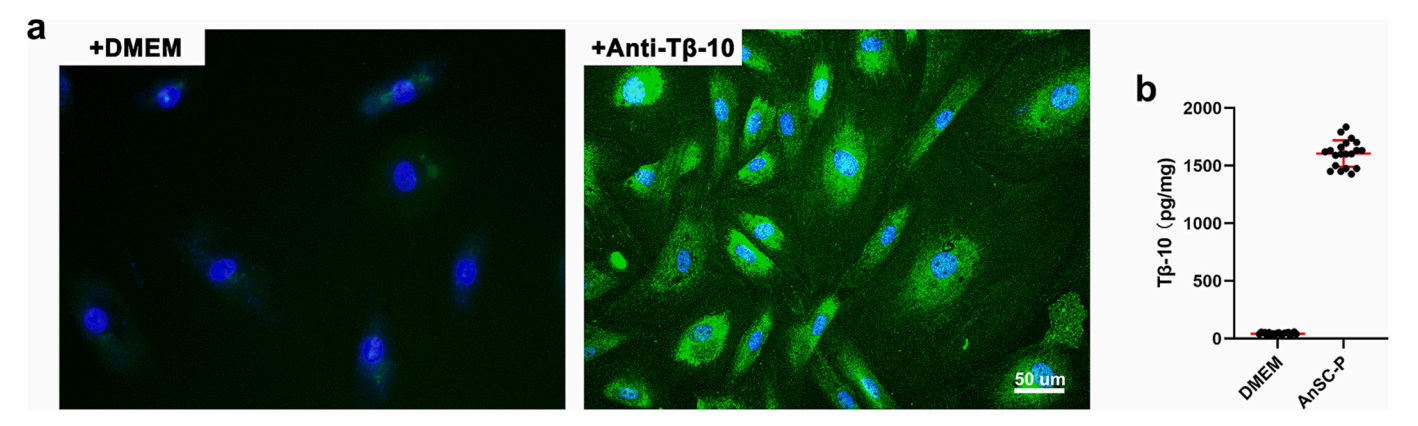


Fig. 2. T $\beta$ -10 expression status in the AnSCs. (a) Detected via immunofluorescence, note that AnSCs highly expressed T $\beta$ -10. (b) Detected via ELISA assay. Note that T $\beta$ -10 may play a positive role in the anti-fibrosis of AnSC-P treatment. Value: mean  $\pm$  s.e.m.; scale bar = 50 μm. Abbreviation: T $\beta$ -10, Thymosin  $\beta$ -10.

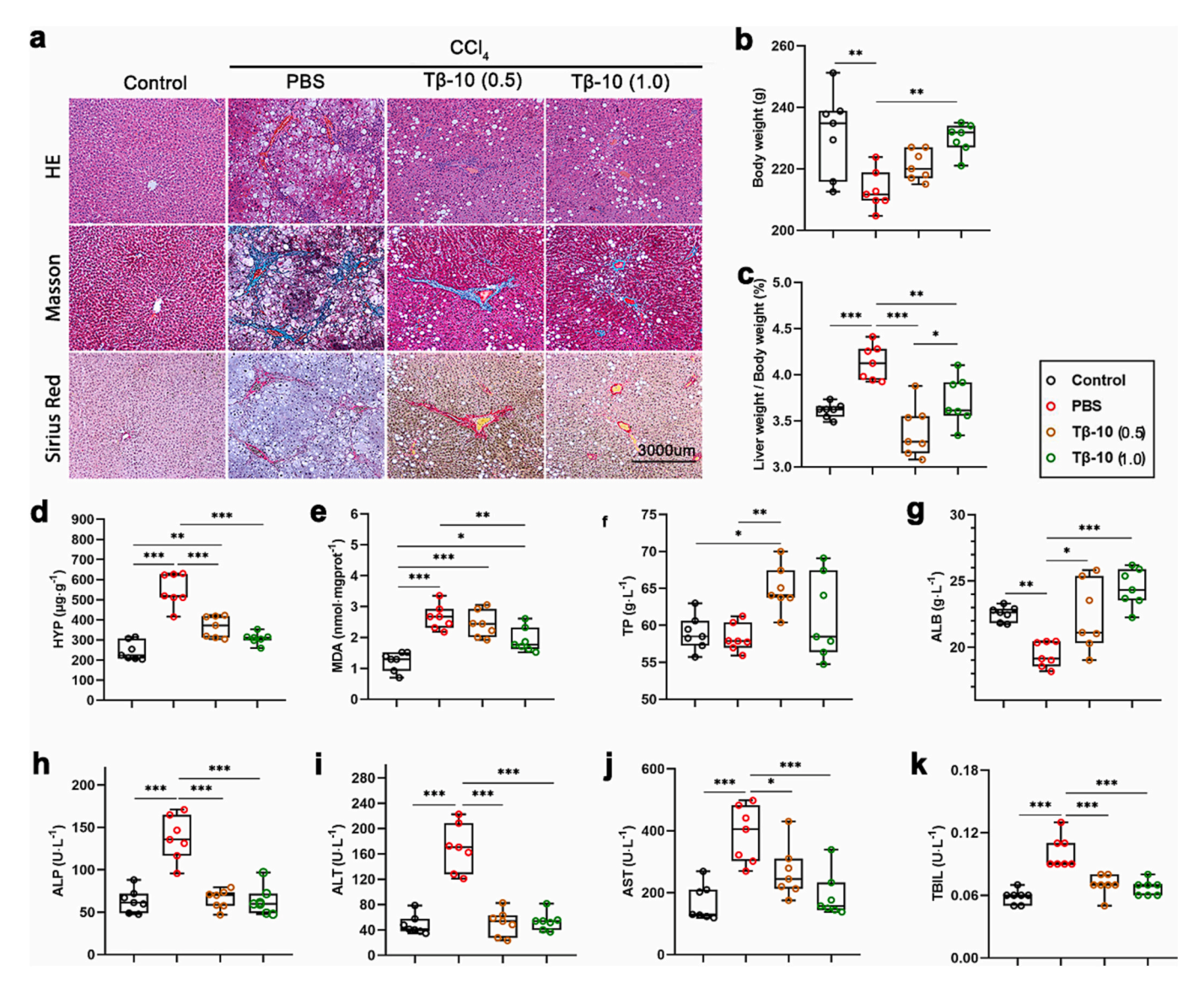


Fig. 3. Effects of Tβ-10 on rat liver fibrosis induced by CCl<sub>4</sub>. For the treatment and group allocation, refer to Fig. 1: Control, PBS, Tβ-10 (0.5 mg/kg), Tβ-10 (1.0 mg/kg). (a) Photomicrographs of liver sections with staining of HE, Masson or Sirius Red; scale bar = 3000 μm. (b) Bodyweight. (c) Liver weight/bodyweight. (d,e) Concentration of liver HYP and MDA. (f-k) Serum biochemical parameters (TP, ALB, ALP, ALT, AST, and TBIL) related to liver function. Note that Tβ-10 treatment significantly suppressed liver fibrosis and improved liver function compared with the PBS group in a dose-dependent manner. Value: mean  $\pm$  s.e.m.; \*p < 0.05, \*\*p < 0.01, and \*\*\*p < 0.001 by one-way ANOVA. (For interpretation of the references to color in this figure legend, the reader is referred to the web version of this article.)

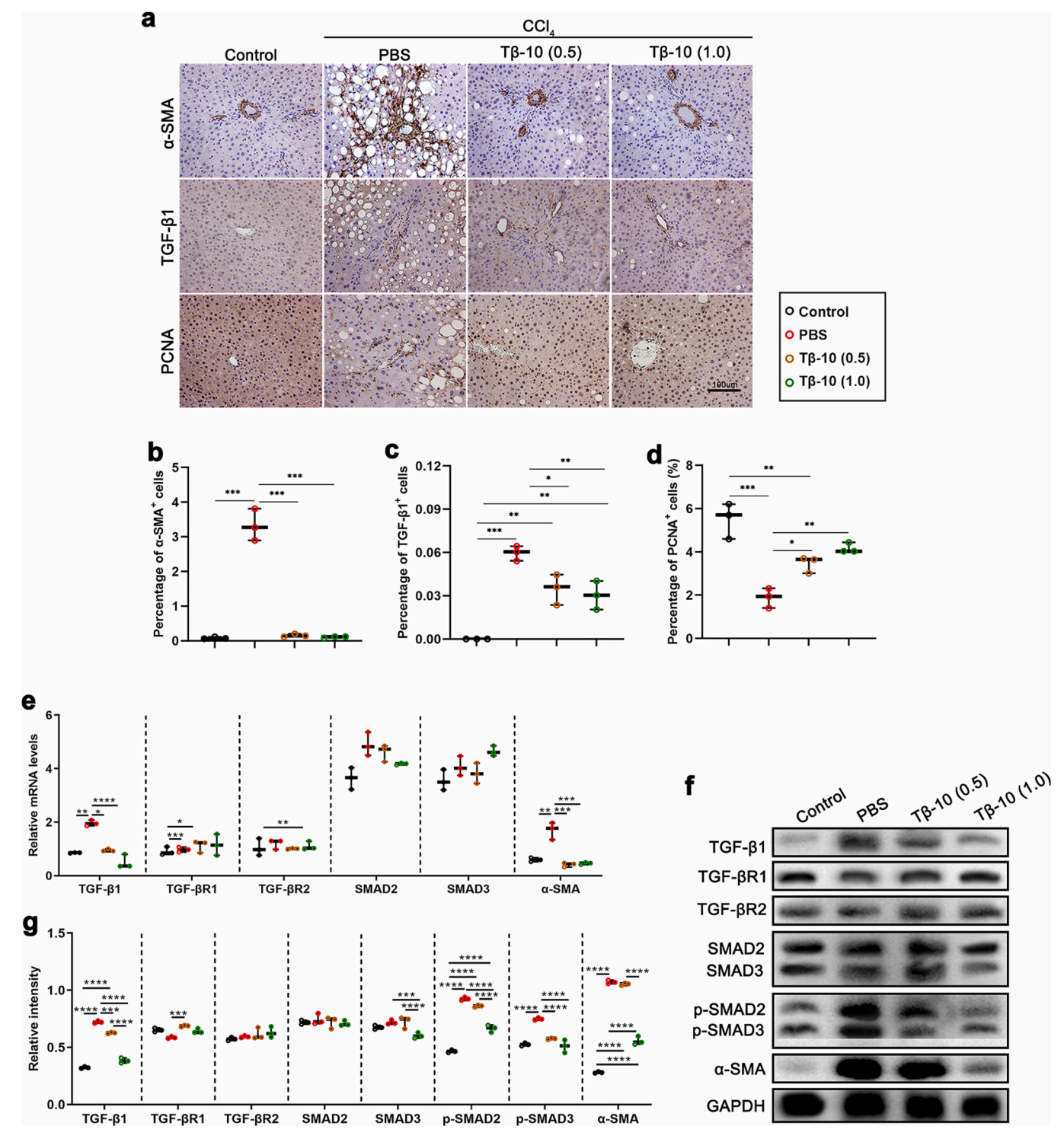
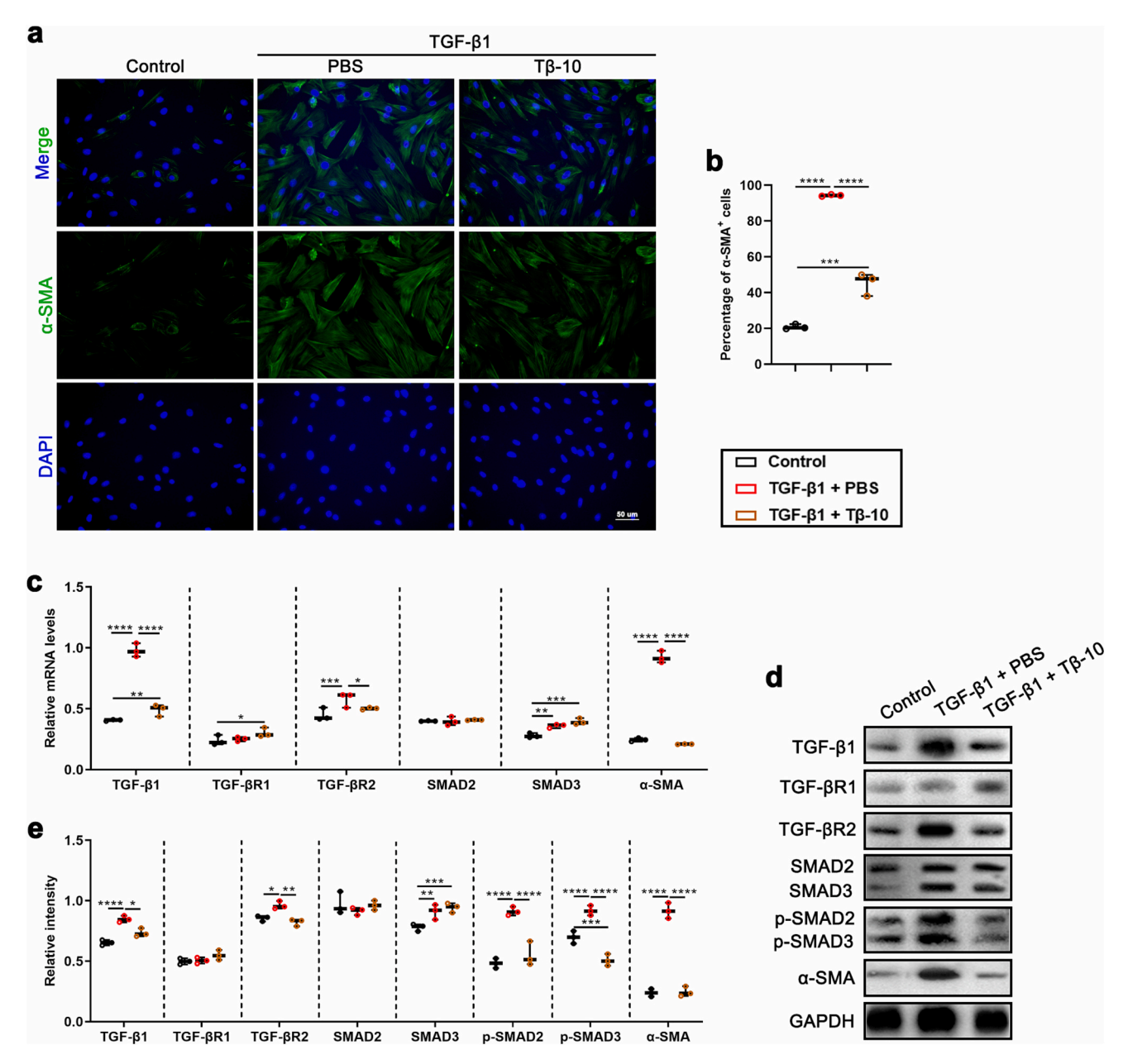


Fig. 4. Effects of Tβ-10 on the expression of TGF-β1/SMAD signaling pathway-related genes in rat liver tissue. (a) Photomicrographs of liver sections staining with immunohistochemistry ( $\alpha$ -SMA, TGF- $\beta$ 1, and PCNA); scale bar = 100 μm. (b-d) Percentage of  $\alpha$ -SMA<sup>+</sup>, TGF- $\beta$ 1<sup>+</sup> or PCNA<sup>+</sup> cells calculated based on the immunohistochemical staining. € Relative mRNA levels of TGF- $\beta$ 1, TGF- $\beta$ R1, TGF- $\beta$ R2, SMAD2, SMAD3, and  $\alpha$ -SMA. (f) Expression levels of TGF- $\beta$ 1, TGF- $\beta$ R1, TGF- $\beta$ R2, SMAD2, SMAD3, pSMAD2, pSMAD3,  $\alpha$ -SMA, and GAPDH. (g) Relative intensity of protein analyzed based on western blot images using Image J Software. Note that Tβ-10 promoted hepatocyte regeneration and down-regulated the expressions of TGF- $\beta$ 1/SMAD signaling pathway-related genes in vivo. Value: mean ± s.e.m.; \*p < 0.05, \*\*p < 0.01, \*\*\*p < 0.001, and \*\*\*\*\*p < 0.0001 by one-way ANOVA. TGF- $\beta$ 1, transforming growth factor  $\beta$ 1; TGF- $\beta$ R1, transforming growth factor  $\beta$ 1 receptor 1; TGF- $\beta$ R2, transforming growth factor  $\beta$ 1 receptor 2; SMAD2, drosophila mothers against decapentaplegic protein 2; pSMAD3, phosphorylated drosophila mothers against decapentaplegic protein 3; pSMAD2, phosphorylated drosophila mothers against decapentaplegic protein 3; PCNA, proliferating cell nuclear antigen; α-SMA, α-smooth muscle actin; GAPDH, glyceraldehyde-3-phosphate dehydrogenase.



**Fig. 5.** Effects of Tβ-10 on HSC activation induced by TGF- $\beta$ 1- in vitro. TGF- $\beta$ 1 was added to the HSCs after 48 h culture to induce activation; at the same time, Tβ-10 was treated to the cells, then the expression level of α-SMA was detected using immunofluorescence staining (**a,b**), and the expression levels of TGF- $\beta$ 1/SMAD signaling pathway-related genes were detected using qRT-PCR (**c**) and western blot assay (**d, e**). Note that Tβ-10 inhibited TGF- $\beta$ 1-induced HSC activation and down-regulated the expressions of TGF- $\beta$ 1/SMAD signaling pathway-related genes in vitro. Value: mean  $\pm$  s.e.m.; \*p < 0.05, \*\*p < 0.01, \*\*\*p < 0.001, and \*\*\*\*p < 0.0001 by one-way ANOVA; scale bar = 50 μm. HSC, hepatic stellate cell.

following antibodies at 4 °C overnight: anti-TGF- $\beta$ 1 (Bioss, bsm-33,345 M, Beijing, China, 1: 2000 dilution), anti-TGF- $\beta$ R1 (Bioss, bs-0638R, Beijing, China, 1: 2000 dilution), anti-TGF- $\beta$ R2 (Bioss, BS-0117R, Beijing, China, 1: 2000 dilution), anti-SMAD2 (Beyotime, AF1300, Shanghai, China, 1: 2000 dilution), anti-SMAD3 (Beyotime, AF1501, Shanghai, China, 1: 2000 dilution), anti-pSMAD2 + pSMAD3 (Beyotime, AF5920, Shanghai, China, 1: 2000 dilution), anti- $\alpha$ -SMA (ProteinTech, 14395-1-AP, Wuhan, China, 1: 3000 dilution), and anti-GAPDH (Beyotime, AF2819, Shanghai, China, 1: 2000 dilution). Membranes were then incubated with the secondary antibody coupled with horseradish peroxidase. Levels of proteins were detected using an ECL system. Western blot analyses were performed in triplicate and the target protein bands were quantified using Image-J software and normalized using the intensity of GAPDH.

# 2.10. Statistical analysis

All data are presented as mean  $\pm$  s.e.m. (n  $\geq$  3). Statistical analysis was conducted using Graphpad Prism software with a one-way ANOVA; \*p < 0.05, \*\*p < 0.01, \*\*\*p < 0.001, or \*\*\*\*p < 0.0001 was considered statistically significant or highly significant.

# 3. Results

# 3.1. AnSC-P treatment reduced rat liver fibrosis induced by CCl<sub>4</sub>

The rats with liver fibrosis were treated with AnSC-P. The results showed that after 4 weeks of treatment, AnSC-P reduced the thickness of central venous walls, fibrous hyperplasia, inflammatory cell infiltration, collagen deposition, and fat degeneration in the fibrotic liver (Fig. 1a).

AnSC-P treatment also resulted in an increase in bodyweight and liver index (liver weight/bodyweight) of the fibrotic rats compared with the PBS control (Fig. 1b, c). Furthermore, AnSC-P treatment significantly decreased the concentrations of HYP (p < 0.0001) and MDA (p < 0.001) in the liver tissue compared to the PBS treatment (Fig. 1d, e); decreased the levels of serum ALP, ALT, AST and TBIL, and increased the levels of serum TP and ALB to varying degrees compared to the PBS treatment (Fig. 1f–k). Notably, AnSC-P was more effective than BMSC-P in alleviating liver fibrosis and improving liver function. These results suggest that AnSC-P can play a positive role in reducing liver fibrosis.

# 3.2. AnSC-P reduction in liver fibrosis may be effected by the diffusible molecule, $T\beta$ -10

Our previous study found that AnSCs highly express a low molecular weight polypeptide, Tβ-10 [20,23], which was also confirmed in this study (Fig. 2a), and we found that  $T\beta$ -10 is a highly enriched substance in AnSC-P (Fig. 2b); thus, we speculated that  $T\beta$ -10 may be a key component of AnSC-P with anti-fibrotic activity. The rats with fibrotic livers were treated with two doses of T $\beta$ -10. Results showed that T $\beta$ -10 significantly reduced the thickness of central venous walls, fibrous hyperplasia, inflammatory cell infiltration, and collagen deposition, in a dose-dependent manner (Fig. 3a). Tβ-10 also significantly increased bodyweight and liver index (liver weight/bodyweight) of the rats with fibrotic livers compared to the PBS control (Fig. 3b, c; p < 0.01). Furthermore, Tβ-10 treatment significantly decreased the concentrations of HYP (p < 0.001) and MDA (p < 0.01) in the liver tissue (Fig. 3d, e) and the serum levels of ALP, ALT, AST and TBIL in a dose-dependent manner compared with the PBS treatment; in contrast, the serum levels of TP and ALB significantly increased (Fig. 3f-k). These results suggest that AnSC-P effectively reduced liver fibrosis and that this may be achieved, at least partially, via  $T\beta$ -10.

# 3.3. T $\beta$ -10 reduced liver fibrosis, possibly via down-regulating TGF- $\beta$ 1/SMAD pathway

Next, we explored the possible mechanism of T $\beta$ -10 in reducing liver fibrosis. The histological results showed that the two doses of T $\beta$ -10 treatment significantly decreased expression levels of both  $\alpha$ -SMA (p < 0.001 and p < 0.001) and TGF- $\beta$ 1 (p < 0.05 and p < 0.001), while increasing the expression levels of PCNA (p < 0.05 and p < 0.01) compared to the PBS treatment (Fig. 4a–d). QRT-PCR results showed that T $\beta$ -10 treatment significantly decreased the expression levels of genes related to the TGF- $\beta$ 1/SMAD signaling pathway (TGF- $\beta$ 1, TGF- $\beta$ R1, TGF- $\beta$ R2, and  $\alpha$ -SMA) (Fig. 4e; p < 0.05) in the fibrotic liver tissues of rats. Similar results were achieved using western blot analysis where T $\beta$ -10 treatment significantly decreased the expression levels of TGF- $\beta$ 1, TGF- $\beta$ R1, SMAD3, p-SMAD2, p-SMAD3, and  $\alpha$ -SMA in a dose-dependent manner (Fig. 4f, g; p < 0.05). These results suggest that the effect of T $\beta$ -10 in reducing liver fibrosis may be via down-regulation of the TGF- $\beta$ 1/SMAD signaling pathway and promotion of normal hepatocyte division.

# 3.4. $T\beta$ -10 inhibited TGF- $\beta$ 1-induced HSC activation in vitro

To further verify the forgoing results, we carried out an in vitro study, in which T $\beta$ -10 was added to the HSC (+TGF- $\beta$ 1) culture system to determine whether this could directly affect HSC activation (the expression of  $\alpha$ -SMA [8]). The results showed that T $\beta$ -10 treatment inhibited TGF- $\beta$ 1-induced expression level of  $\alpha$ -SMA (Fig. 5a, b). Moreover, the mRNA levels of the genes involved in the TGF- $\beta$ 1/SMAD signaling pathway (TGF- $\beta$ 1, TGF- $\beta$ R1, TGF- $\beta$ R2, SMAD3 and  $\alpha$ -SMA) were all down-regulated by the T $\beta$ -10 treatment (Fig. 5c). Similar results were achieved using the western blot analysis where T $\beta$ -10 treatment significantly decreased the expression levels of TGF- $\beta$ 1, TGF- $\beta$ R2, SMAD3, p-SMAD2, p-SMAD3, and  $\alpha$ -SMA (Fig. 5d, e; p < 0.05). Overall, our results suggest that the effect of T $\beta$ -10 in reducing liver fibrosis may

be achieved via inhibition of HSC activation.

#### 4. Discussion

Initiation of liver fibrosis has been attributed to the persistent and excessive activation of HSCs, which secrete abundantly extracellular matrix proteins that generate the fibrous scar [1,2,6]. This is essentially the same as the scar-associated healing of cutaneous wounds, both of which are a result of excessive fibrosis. However, the fibrogenic process in tissues with wound scarring after injury is still considered inevitable. However, a wound of 10 cm or larger in diameter on top of the deer pedicle (permanent bony protuberances from which antlers are cast and regenerate) heals rapidly (within two weeks) and leaves almost no visible scar [12,13]. This system, therefore, offers a rare opportunity to seek understanding of anti-fibrotic healing in mammals.

In this respect, firstly, we sought to understand how this potential for non-fibrotic healing may be affected. We have found that it is the closely-adjacent AnSCs, resident in the antler blastema, that provide the pedicle wound skin with the ability to achieve non-fibrotic healing through a paracrine manner; hence, the peptides of AnSCs may be the candidates for the role [24]. Secondly, AnSC-induced non-fibrotic wound healing is not species-specific and we have shown that healing of wounds in rats may be achieved via treatment with AnSCs or the AnSC-derived components [14–17]. Thirdly, the anti-fibrotic effect of AnSCs is not tissue-specific as shown in the successful treatment of pulmonary fibrosis and liver fibrosis in rats via treatment with AnSCs [18,19]. Considering the potential risks of direct transplantation of xenogeneic animal stem cells, it is necessary to identify specific components of AnSCs that may play such an anti-fibrotic role.

In this study, we isolated the peptides from the AnSCs (extracellular and intracellular) and evaluated the effect of this peptide combination (AnSC-P) on liver fibrosis in our rat model. Undoubtedly, the components of AnSC-P are very complex, including proteins, polypeptides and nucleic acid substances, and these components may well stimulate an immune response, if applied in a clinical treatment. If a monomeric polypeptide with anti-fibrotic potential could be identified from the AnSC-P components, it would provide a potential approach to clinical application. Coincidentally, we have found previously that Tβ-10, a low molecular weight polypeptide that is highly expressed in AnSCs [20], is also highly enriched in AnSC-P.  $T\beta$ -10 is differentially expressed in embryogenesis and neurogenesis [25,26], and is known to play important roles in cell movement [27], angiogenesis [28], cell growth and apoptosis [29]. Therefore, given there is a case to consider its potential in the treatment of some disease conditions [30,31], we evaluated its effects in the present study.

As expected, AnSC-P significantly reduced liver fibrosis. In some aspects, the effects were more potent than the control BMSC-P. To the best of our knowledge, this is the first study to demonstrate the effects of AnSC-P and their main component, T $\beta$ -10, on rat liver fibrosis in vivo and HSC activation in vitro. We found that AnSC-P effectively reduced liver fibrosis in our rat model, which may have been effected via T $\beta$ -10. In addition, T $\beta$ -10 also inhibited TGF- $\beta$ 1-induced HSC activation. Furthermore, both in vivo and in vitro, the effects were achieved by inhibition of the TGF- $\beta$ 1/SMAD signaling pathway. Therefore, we propose that T $\beta$ -10 could offer a valid approach for the treatment of liver fibrosis in the clinical setting.

Our previous studies have shown that the protein structure of antler T $\beta$ -10 is more flexible than that in other species, which might provide opportunities for the antler-derived peptide to interact with other functional proteins [28]. The present results showed that both AnSC-P and T $\beta$ -10 significantly reduced liver fibrosis. In addition, given the specific structure of antler T $\beta$ -10, it is speculated that it may have a stronger anti-fibrotic activity than other species, because it may bind more efficiently to the protein that activates HSCs, thus inhibiting its function.

Many factors are known to be involved in the activation of HSC, such

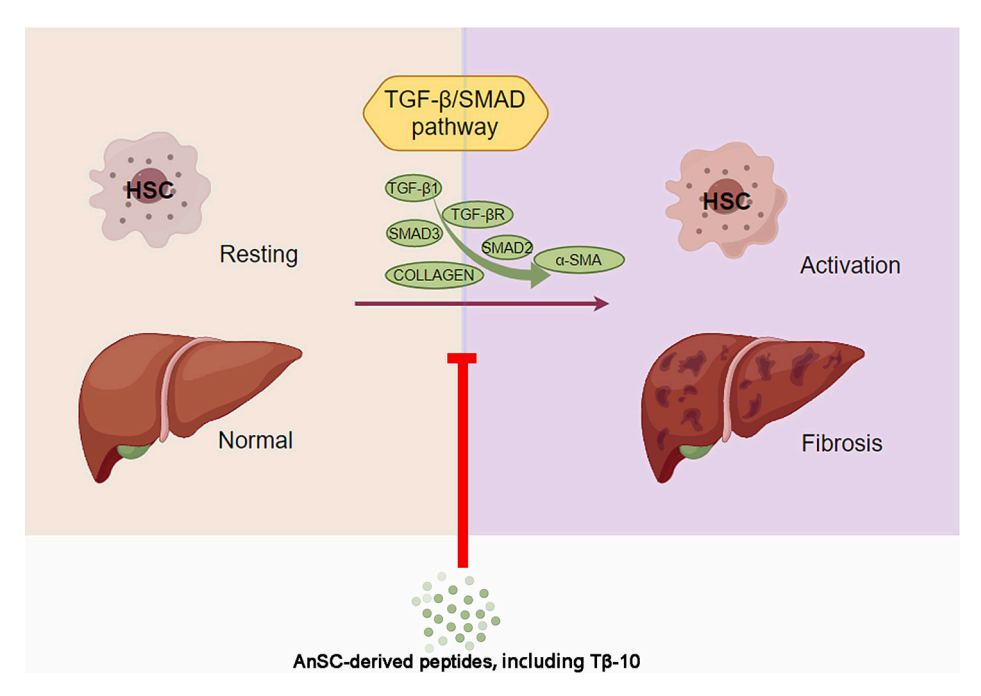


Fig. 6. Schematic to illustrate that antler stem cell-derived peptide,  $T\beta$ -10, reduces liver fibrosis and HSC activation via inhibiting the TGF- $\beta$ 1/SMAD signaling pathway.

as mitogen-activated protein kinase (MAPK), growth factors, leptin, and TGF-β1 [2,6]. Amongst these factors, TGF-β1 is the most critical one [32]. TGF-\beta1 exerts its biological effects through activation of downstream genes SMAD2/3, which then become phosphorylated and oligomerized with SMAD4. The complex is then translocated into the nucleus to regulate the expression of fibrosis-related genes. In the present study, we found that Tβ-10 treatment effectively decreased the expression levels of genes related to the TGF-β1/SMAD signaling pathway, especially TGF-β1, pSMAD2, and pSMAD3 in liver tissue of CCl<sub>4</sub>-induced liver fibrosis in vivo and TGF-β1-induced HSC activation in vitro. It is important to note that our study was only conducted in rats and has not been extended to other animals. At the same time, it is also to conduct relevant toxicological tests (although Chinese people have consumed antler products for thousands of years without any adverse effects). In future work, we will carry out in-depth research on these two aspects and try to push the anti-fibrosis effect of  $T\beta$ -10 to the clinic.

## 5. Conclusion

The application of T $\beta$ -10 effectively reduced rat liver fibrosis in vivo and inhibited HSC activation in vitro, and the effect may be achieved through down-regulating the TGF- $\beta$ 1/SMAD signaling pathway (Fig. 6). Overall, we propose that there is a case to investigate T $\beta$ -10 as a novel drug candidate for the treatment of liver fibrosis in the clinical setting.

# CRediT authorship contribution statement

Guokun Zhang: Conceptualization, Methodology, Writing – original draft, Writing – review & editing, Data curation. Liyan Shi: Methodology, Writing – original draft, Data curation. Jiping Li: Methodology. Jing Ren: Methodology. Dongxu Wang: Methodology. Xin Guo: Investigation, Methodology, Supervision. Qianqian Guo: Conceptualization, Investigation, Supervision. Chunyi Li: Conceptualization, Writing – review & editing.

# Declaration of competing interest

The authors declare that they have no known competing financial

interests or personal relationships that could have appeared to influence the work reported in this paper.

## Data availability

All datasets generated and analyzed during this study are included in this published paper and its Supplementary Information files.

# Acknowledgements

This work was supported by the National Natural Science Foundation of China (Grant No. U20A20403, 32300708), the Natural Science Foundation of Jilin Province (Grant No. YDZJ202301ZYTS508, YDZJ202201ZYTS435), the Independent Innovation Capacity Construction Project of Jilin Province (Grant No. 2022C013), the Doctoral Research Start-Up Fund of Changchun Sci-Tech University (Grant No. 202303, 202304) and the Young Scientific and Technological Talents Support Project of Jilin Province (Grant No. QT202203). We also thank Dr. Peter Fennessy for his critique of the manuscript and valuable suggestions, and the Jilin Dongao Deer Industry Group Co. Ltd. for providing deer antlers for the in vitro study.

# Appendix A. Supplementary data

Supplementary data to this article can be found online at https://doi.org/10.1016/j.ijbiomac.2024.130502.

# References

- T. Kisseleva, D. Brenner, Molecular and cellular mechanisms of liver fibrosis and its regression, Nat. Rev. Gastroenterol. Hepatol. 18 (3) (2021) 151–166.
- [2] V. Hernandez-Gea, S.L. Friedman, Pathogenesis of liver fibrosis, Annu. Rev. Pathol. 6 (2011) 425–456.
- [3] S.L. Friedman, Transcriptional regulation of stellate cell activation, J. Gastroenterol. Hepatol. 21 (s3) (2006) S79–S83.
- [4] X. Wu, X. Wu, Y. Ma, F. Shao, Y. Tan, T. Tan, L. Gu, Y. Zhou, B. Sun, Y. Sun, CUG-binding protein 1 regulates HSC activation and liver fibrogenesis, Nat. Commun. 7 (2016) 13498
- [5] A. Woodhoo, M. Iruarrizagalejarreta, N. Beraza, J.L. Garcíarodríguez, N. Embade, D. Fernándezramos, N. Matinezlopez, V. Gutiérrez, B. Arteta, J. Caballeria, HuR contributes to hepatic stellate cell activation and liver fibrosis, Hepatology 56 (5) (2012) 1870.

- [6] L. Hammerich, F. Tacke, Hepatic inflammatory responses in liver fibrosis, Nat. Rev. Gastroenterol. Hepatol. 20 (10) (2023) 633–646.
- [7] N.C. Henderson, T.D. Arnold, Y. Katamura, M.M. Giacomini, J.D. Rodriguez, J. H. Mccarty, A. Pellicoro, E. Raschperger, C. Betsholtz, P.G. Ruminski, Targeting of αv integrin identifies a core molecular pathway that regulates fibrosis in several organs, Nat. Med. 19 (12) (2013) 1617–1624.
- [8] T. Tsuchida, S.L. Friedman, Mechanisms of hepatic stellate cell activation, Nat. Rev. Gastroenterol. Hepatol. 14 (7) (2017) 397–411.
- [9] M. Krampera, K. Le Blanc, Mesenchymal stromal cells: putative microenvironmental modulators become cell therapy, Cell Stem Cell 28 (10) (2021) 1708–1725.
- [10] N. Song, M. Scholtemeijer, K. Shah, Mesenchymal stem cell immunomodulation: mechanisms and therapeutic potential, Trends Pharmacol. Sci. 41 (9) (2020) 653–664.
- [11] T. Qin, G. Zhang, Y. Zheng, S. Li, Y. Yuan, Q. Li, M. Hu, H. Si, G. Wei, X. Gao, X. Cui, B. Xia, J. Ren, K. Wang, H. Ba, Z. Liu, R. Heller, Z. Li, W. Wang, J. Huang, C. Li, Q. Qiu, A population of stem cells with strong regenerative potential discovered in deer antlers, Science 379 (6634) (2023) 840–847.
- [12] C. Li, W. Chu, The regenerating antler blastema: the derivative of stem cells resident in a pedicle stump, Front. Biosci. (Landmark Ed.) 21 (3) (2016) 455–467.
- [13] C. Li, J.M. Suttie, D.E. Clark, Morphological observation of antler regeneration in red deer (Cervus elaphus), J. Morphol. 262 (3) (2004) 731–740.
- [14] X. Rong, W. Chu, H. Zhang, Y. Wang, X. Qi, G. Zhang, Y. Wang, C. Li, Antler stem cell-conditioned medium stimulates regenerative wound healing in rats, Stem Cell Res Ther 10 (1) (2019) 326.
- [15] G.K. Zhang, J. Ren, J.P. Li, D.X. Wang, S.N. Wang, L.Y. Shi, C.Y. Li, Injectable hydrogel made from antler mesenchyme matrix for regenerative wound healing via creating a fetal-like niche, World J. Stem Cells 15 (7) (2023) 768–780.
- [16] G. Zhang, D. Wang, J. Ren, H. Sun, J. Li, S. Wang, L. Shi, Z. Wang, M. Yao, H. Zhao, C. Li, Velvet antler peptides reduce scarring via inhibiting the TGF-β signaling pathway during wound healing, Front. Med. (Lausanne) 8 (2021) 799789.
- [17] X. Rong, G. Zhang, Y. Yang, C. Gao, W. Chu, H. Sun, Y. Wang, C. Li, Transplanted antler stem cells stimulated regenerative healing of radiation-induced cutaneous wounds in rats, Cell Transplant. 29 (2020) 963689720951549.
- [18] G. Zhang, L. Shi, J. Li, S. Wang, J. Ren, D. Wang, P. Hu, Y. Wang, C. Li, Antler stem cell exosomes alleviate pulmonary fibrosis via inhibiting recruitment of monocyte macrophage, rather than polarization of M2 macrophages in mice, Cell Death Dis. 9 (1) (2023) 359.

- [19] X. Rong, Y. Yang, G. Zhang, H. Zhang, C. Li, Y. Wang, Antler stem cells as a novel stem cell source for reducing liver fibrosis, Cell Tissue Res. 379 (1) (2020) 195–206
- [20] W. Zhang, W. Chu, Q. Liu, D. Coates, Y. Shang, C. Li, Deer thymosin beta 10 functions as a novel factor for angiogenesis and chondrogenesis during antler growth and regeneration, Stem Cell Res Ther 9 (1) (2018) 166.
- [21] G. Zhang, Y. Jiang, X. Liu, Y. Deng, B. Wei, L. Shi, Lingonberry anthocyanins inhibit hepatic stellate cell activation and liver fibrosis via TGFβ/Smad/ERK signaling pathway, J. Agric. Food Chem. 69 (45) (2021) 13546–13556.
- [22] L. Shi, X. Zhang, X. Liu, Y. Jiang, Y. Deng, J.J.F.B. Liu, Cranberry (Vacinium macrocarpon) Phytochemicals Inhibit Hepatic Stellate Cell Activation and Liver Fibrosis 42, 2021, p. 42.
- [23] S. Deb-Choudhury, W. Wang, S. Clerens, C. McMahon, J.M. Dyer, C. Li, Direct localisation of molecules in tissue sections of growing antler tips using MALDI imaging, Mol. Cell. Biochem. 409 (1–2) (2015) 225–241.
- [24] C. Li, F. Yang, G. Li, X. Gao, X. Xing, H. Wei, X. Deng, D.E. Clark, Antler regeneration: a dependent process of stem tissue primed via interaction with its enveloping skin, J. Exp. Zool. A Ecol. Genet. Physiol. 307 (2) (2007) 95–105.
- [25] P. Carpintero, F. Franco del Amo, R. Anadón, J. Gómez-Márquez, Thymosin beta10 mRNA expression during early postimplantation mouse development, FEBS Lett. 394 (1) (1996) 103–106.
- [26] S.C. Lin, M. Morrison-Bogorad, Developmental expression of mRNAs encoding thymosins beta 4 and beta 10 in rat brain and other tissues, J. Mol. Neurosci. 2 (1) (1990) 35–44.
- [27] S.C. Lin, M. Morrison-Bogorad, Cloning and characterization of a testis-specific thymosin beta 10 cDNA. Expression in post-meiotic male germ cells, J. Biol. Chem. 266 (34) (1991) 23347–23353.
- [28] H. Ba, D. Wang, TO. Yau, Y. Shang, C. Li, Transcriptomic analysis of different tissue layers in antler growth center in sika deer (Cervus nippon), BMC Genomics 20 (1) (2019) 173.
- [29] A.K. Hall, Thymosin beta-10 accelerates apoptosis, Cell. Mol. Biol. Res. 41 (3) (1995) 167–180.
- [30] S. Sribenja, M. Li, S. Wongkham, C. Wongkham, Q. Yao, C. Chen, Advances in thymosin beta10 research: differential expression, molecular mechanisms, and clinical implications in cancer and other conditions, Cancer Investig. 27 (10) (2009) 1016–1022.
- [31] J. Gomez-Marquez, R. Anadon, The beta-thymosins, small actin-binding peptides widely expressed in the developing and adult cerebellum, Cerebellum (London, England) 1 (2) (2002) 95–102.
- [32] R. Bataller, D.A. Brenner, Liver fibrosis, J. Clin. Invest. 115 (2) (2005) 209-218.